A STUDY OF THE ELECTRON EXCITED H_2 LYMAN BAND SYSTEM FROM CASCADE TRANSITIONS

D. DZICZEK
J. AJELLO
G. JAMES
D. HANSEN

JET PROPULSION LABORATORY
CALIFORNIA INSTITUTE OF TECHNOLOGY
PASADENA, CA 91109

SUBMITTED TO:

PHYSICAL REVIEW LETTERS

JUNE 15, 1999

ABSTRACT

The intensity of UV resonance transitions excited by electron impact is determined by direct and cascade processes. The lifetime of decay by spontaneous emission is short (<10 ns); the lifetimes for cascade from higher-lying states is longer (>30 ns). To measure the electron impact cascade spectrum of the Lyman band system of H_2, we use the long lifetimes for cascade pumping from higher lying states. Pulsing the electron gun and gating the photon detector to measure the cascade spectrum, after the directly excited population decays, allows a determination of the cross section from cascading.

PACS No. 34.50.Gb, 34.80.Gs: Atomic and Molecular Collision Processes and Interaction

The steady state intensity of UV resonance transitions in atoms and molecules excited by electron impact is determined by direct and cascade processes. Direct and cascade processes are difficult to separate experimentally and to calculate theoretically. The Lyman band system ($B\ ^1\Sigma_u^+ - X\ ^1\Sigma_g^+$) is the most intense of the H_2 band systems (Liu et al., 1998). To date the magnitude of the EF,GK, $H\ ^1\Sigma_g^+ \rightarrow B\ ^1\Sigma_u^+$ electron impact cascade contribution to the Lyman band system emission spectrum has eluded theorists and astrophysicists. The principal difficulty lies in understanding the optically-forbidden excitation to the rovibronic levels of the double-minimum gerade states from the $X\ ^1\Sigma_g^+$ ground state. For other species at low electron energies the magnitude of the cascade cross section contribution to an emission cross section of a resonance transition can approach 50% as has been inferred for the OI(130.4 nm) multiplet from electron excitation of O (Meier et al., 1991) and 27% as modeled for the HI(121.6 nm) transition from electron excitation of H (James et al., 1997). The technique demonstrated in this experiment for the H_2 Lyman bands establishes a method for measuring cascade emission cross sections and observing optically-thin cascade spectra, without contamination from the directly excited spectra. The significant result for the Lyman band system is that the cross sections for direct excitation and cascade are nearly equal at 20 eV.

The Lyman Band system is very important in astrophysics since it is a measure of energy input to an astronomical object: the Jupiter aurora (Ajello et al., 1998) and other outer planets (Broadfoot et al.,1981,1989) or Herbig–Haro objects in the interstellar medium (ISM) (Raymond et al., 1997). Collisional excitation of H_2 by electrons results in UV emission from the Rydberg band systems spanning the spectral range 75-170nm. We have measured and modeled this spectrum for many years (Ajello et al., 1984, 1988; Liu et al., 1995; Jonin et al., 1999). Giant strides in modeling high resolution laboratory spectra were made possible in the last few years using the transition probability calculations of Abgrall and co-workers (1994) for the two Rydberg series of H_2: $^1\Sigma_u^+ 1s\sigma np\sigma$ (B, B', n=2, 3)$\rightarrow X\ ^1\Sigma_u^+$ and $^1\Pi_u^+ 1s\sigma np\pi$ (C, D, n=2, 3)$\rightarrow X\ ^1\Sigma_u^+$. The contribution of cascade to the H_2 UV spectrum is only important for the B-state. Its contribution to the Lyman band portion of the Rydberg bands has been estimated based upon Franck-Condon factors and Honl-London factors (Shemansky et al., 1985; Ajello et al., 1988). However, precise calculation is not yet possible because of the many cascade states involved with a complication that each state is perturbed by strong rovibronic coupling. The intensity of the cascade spectrum depends on the total cascade cross section for all contributing states. The previous results indicated about 10% cascade contribution at 100 eV electron impact energy (Ajello et al., 1988). This contribution will increase dramatically with decreasing energy near the threshold energy region (11-20 eV), since the cross section of the optically-forbidden excitation (a combination of quadrupole interaction and static electron exchange) peaks near 18-20 eV for EF→B (Watson and Anderson, 1977).

The main technique to distinguish two channels producing excitation of a specific state is coincidence spectroscopy, which generally employs a DC operation mode (McDaniel, 1989, Khakoo et al., 1996). Signal levels are weak and calibration techniques to obtain integral cross sections are difficult. However, the two direct and cascade channels contributing to a UV resonance spectrum can be conveniently separated in the time domain. Lifetimes of the $B\ ^1\Sigma_u^+$ rovibronic levels are in the range 0.5-2 ns (Abgrall

et al., 1994), whereas the lifetimes of the low vibronic levels of the EF state are 100-1000 ns (Chandler and Thorne, 1986; Glass-Maujean, 1983). The lifetimes of the vibronic levels of the GK, H states are shorter, 30-100 ns (Maujean et al., 1984; Tsukiyama, K. et al., 1992). We show in Fig. 1 a schematic of the two principal gerade states that radiatively cascade in the middle ultraviolet (MUV) and visible/IR to the B $^1\Sigma_u^+$ rovibronic levels. The mutual coupling interactions of the first five gerade states have been studied by Wolniewicz and Dressler (1994). The low v' levels of the B $^1\Sigma_u^+$ state are populated through cascade by dozens of rovibronic levels from each of the GK,H and EF states. The cumulative effect of the slow cascade to a rovibronic level can be studied by monitoring a single fine structure B→X line after the direct excitation has decayed away.

The experimental system in its conventional steady state DC operating mode has been described before (Liu et al., 1995). The system consists of a 3m high-resolution UV spectrometer ($\frac{\lambda}{\Delta\lambda} = 67000$) and an electron collision chamber in tandem. Electrons generated by a thoriated tungsten filament are accelerated by a magnetically collimated electron gun. The electron beam collides at right angles with a beam of gas effusing from a capillary array hole structure. Optical emissions from the electron-excited H_2 are dispersed by a 3 m spectrometer with a 1200 line/mm grating, coated with a B_4C thin film. The detector is a channel electron multiplier coated with CsI.

To operate the electron beam in the pulsed mode the potential of the first accelerating electrode of the gun (L_1) is varied periodically. Fig. 2a shows the time dependence of the electron impact excitation rate which, we assume, is proportional to the instantaneous electron beam current. At the beginning of the pulsing cycle (t_0) the potential of L_1 is changed from 20-30 V below the potential of the cathode (which completely blocks the electron beam) to a value of 2.5 V above the cathode potential (the gun's standard operating voltage for continuous electron beam mode). Consequently , the electron beam current increases rapidly from zero to a stable value equivalent to the continuous beam mode (typically 200 μA within 150 ns). The gun is maintained in this "ON" state for a time sufficient to approach a dynamic equilibrium between excitation and de-excitation processes of the specific target excited state. At time t_1 the potential of L_1 is rapidly reduced to the value below the cathode potential, causing blockage of the electron beam. We have found that a 200 μA electron beam is "turned off" with an instrumental time constant of approximately 30 ns.

Fig 2b shows the expected time dependence of the photon emission rate I(t), following pulsed gun electron impact excitation for both short lifetime (τ <<30 ns, dashed line) and relatively long lifetime ($\tau > 30$ ns) excited states. In general the time dependence of the photon emission rate is the sum of a decay curve corresponding to radiation from the directly excited resonance state and convolutions of decay curves corresponding to all possible cascade channels with the radiative curve of the directly excited state. Additionally, intensity decay curves of all channels are convoluted with the time dependence curve of the electron excitation rate in Fig. 2a.

Fig. 2c depicts the photon gate signal. At the time t_2 the rising edge initiates the counting of photons by the data acquisition system. The falling edge t_3 stops counting shortly before the next period at t_0'. The cross-hatched area in Fig. 2b schematically represents counts from t_2 to t_3.

The pulsing period as well as "beam on" time (t_1-t_0) and gate delay time (t_2-t_1) can be varied in wide range of values, allowing studies of states characterized by effective lifetimes from tens of nanoseconds to approximately 100 μs. There is a 8 μs long lifetime limit associated with excited H_2 molecules at 300 K escaping from the 1.2° x 1.9° field-of –view of this particular optical system. Larger gratings extend the lifetime upper limit.

The signal measured by the counters during a gun pulse is given by,

$$Sig = \int_{t2}^{t3} I(t)dt \qquad (1)$$

$$I(t_2) = -d\,(Sig)/dt \qquad (2)$$

where Sig is the accumulated counts from time, t_2 to t_3. $I(t_2)$ is the intensity of photons at the time of the photon gate pulse transition, obtained by differentiation of the signal.

We show in Fig. 3 a variable gate pulsed-gun lifetime study of one Lyman and one Werner vibrational level. We use a gun period of 3.5 μs with a gun-on duty cycle of 2.0 μs. The gun-on time of five lifetimes for the H_2 v' =1 level of the EF-state, the longest-lived level of interest (Glass-Maujean et al., 1983, 1984), ensures attainment of asymptotic DC conditions for all levels of importance of the EF, GK and H-states by the end of the gun-on pulse. The EF, GK and H-states do not significantly populate any of the Werner levels. For both the gun-on and gun-off part of the cycle, the dashed curve in Fig. 2b schematically represents the intensity of the Werner system. The solid curve in Fig. 2b represents the cascade-driven Lyman band chosen for this study. The photon signal decay curve of the Q1,R0-R4 (1,4)C-X Werner fine structure lines, blended together and measured at 100 eV electron impact energy in the 0.3 nm band pass (FWHM) centered at 115.99 nm, is also shown in Fig. 3. There were no low-lying v' Lyman bands present in the bandpass. The photon decay curve of the R0-R2 (0,4)B-X Lyman fine structure lines measured in a 0.3 nm band pass (FWHM centered at 133.37 nm) at 20 eV electron impact energy is shown in Fig. 3. The difference between the two decay curves is striking. The prompt radiation from the Werner band serves to calibrate the time response of the instrument. The Werner bands contain an insignificant cascade component. The lifetime of the rovibronic levels (v'=1, J'=1) of the C-state is 0.9 ns (Abgrall and Roueff, 1989). The experimental data for the period beginning at the end of the gun-on pulse (t_1 in Fig. 2) were evaluated with a non-linear least-squares curve fitting equation in the form of a sum of two exponential decay curves

$$I(t) = Q_{fast} \exp(-t/\tau_{fast}) + Q_{slow} \exp(-t/\tau_{slow}), \qquad (3)$$

where τ_{fast} and τ_{slow} are the lifetimes of the two strongest channels and Q_{fast} and Q_{slow} are the emission cross sections of the two processes, fast and slow, respectively. The intensity for each process in Eq. 3) is normalized to unity electron flux and gas pressure. The measured lifetime value of τ_{fast} = 30 ns in Fig. 3a for the C-X decay is a measure of the instrumental time constant. This lifetime was also verified by monitoring the time decay of the Faraday cup current when the gun-off pulse occurred. The present experiment cannot distinguish direct excitation and cascade processes that have lifetimes less than 40 ns. It was not the goal of this program to measure the prompt lifetimes of the

direct excitation transition but rather to study the slow cascade late in the decay curve. The Lyman band is analyzed in a similar fashion. The v'=0 level is populated mostly by cascade at 20 eV electron impact energy, with less than 10% direct excitation. The experimental lifetimes were found to be 51 ns for the fast component, and 161 ns for the slow cascade component. A similar lifetime result to within 10% was found for the slow cascade lifetime at 100 eV electron impact energy (not shown). The ratio of the two cross sections (fast/slow) at 20 eV electron impact energy is 0.8 indicating that the slow cascade cross section is stronger. The C-X transition shown in Fig. 2 has a weak secondary process with a lifetime of 184 ns, though its intensity is down a factor of ~ 75 from the direct process. The effect of cascade has been separated from the direct C-X band system. Huber and Herzberg (1979) report several cascade transitions from high Rydberg gerade states: H-C, J-C, K-C. The weak cascade processes are easily detected late in the photon signal decay curve. The explanation of the Lyman decay curve time constants is a weighted average of lifetimes from rovibronic transitions of the n=2 EF and n=3 GK,H states. The strongly excited EF vibrational levels, v'=0,1,2,3 have lifetimes from 139 to 1000 ns (Glass-Maujean et al., 1984, Abgrall, private communication), whereas the strongly excited GK,H levels, v'=0,1,2 have lifetimes of 20-120 ns (Glass-Maujean et al., 1983, Chandler and Thorne, 1986). The n=4 I and J states with lifetimes of 10–20 ns for v'=0 are probably not observed. The excitation cross sections of these states are expected to be small and not contribute significantly to the measured fast lifetime. All of the singlet gerade states are found to exhibit significant J-dependence of lifetimes (Tsukiyama et al., 1992). We interpret the strongest transition in the decay curve as arising mainly from the EF double-minimum state and the weaker and faster decay curve as arising mainly from the GK,H double-minimum states. The strongest vibrational level of the EF state is v'= 0 which dominates the slow cascade lifetime of this experiment. The measured lifetime for v'= 0 is 200 ns for J=0 and 213 ns for J=1(Chandler and Thorne, 1986; Glass-Maujean et al., 1984;). All of the lower vibrational levels of the E-state inner potential well favor decays to the B v' =0 level (Spindler, 1969). The bandpass of the spectrometer also contains a small blend contribution (less than 10% at 20 eV) from the R0,1(5,6) B-X fine structure lines at 133.89,133.43 nm.

The experimental decay curves establish the gate delay time needed to observe a cascade spectrum, free of any directly excited Rydberg bands. At a gate delay time of 135 ns after the gun-off pulse has occurred, the Werner band intensity has decreased by a factor of 40, while the v'=0 Lyman band is down by only a factor of 3 (near e). For a gate delay time of 135 ns we show in Fig. 4 the cascade spectrum of the Lyman bands with a band pass of 0.4 nm. The wavelength threshold is near 90 nm. The UV spectrum from 90-170 nm is calibrated by techniques previously published (Jonin et al., 1999; Liu et al., 1995). The low-resolution wavelength structure in Fig. 4 is indicative of strong v' = 0,1,2-v" progressions. However high vibrational levels (> v' = 35) of the B-state must be weakly excited by cascade in order to explain the full spectrum to 90 nm. The cascade spectrum is compared to the DC electron beam spectrum (cascade + direct) and the Rydberg band system direct spectrum, which we have recently modeled (Jonin et al., 1999). The regression analysis in Fig. 4 establishes the cross section for the sum of all cascade processes. The channel intensities of the experimental cascade spectrum and the direct excitation model spectrum are used mathematically as independent vectors in the regression analysis. The regression analysis determines a linear combination of these

vectors that are summed to fit the steady state spectrum. The best fit is shown in Fig. 4a. The component fits to the DC spectrum are shown in Fig. 4b. The RMS best fit in Fig. 4a is 98% with the major discrepancies occurring at the unmodeled Lyman atomic H lines from dissociative excitation for n>2 (note H Ly β at 102.6 nm). We have calculated the total of all Rydberg emission cross sections from 90-170 nm (which is proportional to the area in the model direct excitation spectrum [dotted curve] of Fig. 4b). Liu et al. (1998) give the direct excitation cross section of the Lyman bands at 20 eV as 2.0×10^{-17} cm^2. Based on the 100 eV Rydberg cross sections by Jonin et al.(1999) and the excitation function by Liu et al., the cross section for the Rydberg bands at 20 eV is established to be 3.90×10^{-17} cm^2. The cascade cross section is proportional to the area under the cascade spectrum (dashed curve, Fig. 4b, excluding H Lα). Thus, the B-X cascade cross section is determined to be 1.7×10^{-17} cm^2 at 20 eV.

The spectral pattern from direct excitation and cascade are different. Direct excitation produces a large population in the B-state centered at v' =7 whereas cascade populates the lower vibrational levels most strongly, beginning at v' = 0. Studying Figure 4b shows that there are clearly regions in the far ultraviolet (FUV) spectrum that are dominated by cascading. The most important two wavelength regions that are exclusively (more than 90%) due to cascade lie near 133-135 nm and 139-142 nm. These regions correspond to the rotational lines of the (0,1) and (0,2) vibrational bands of the B-X Lyman bands, the two strongest bands of the v'=0, v'' progression. The absolute largest intensity in the cascade spectrum occurs at 161 nm and involves the superposition of rovibronic transitions from v' = 4, 5 and 6. Detailed rotational line identifications are given in the H_2 spectral atlas of Roncin and Launay (1994). Recently, James et al. (1998) reported the 19 eV and 100 eV emission cross sections of the GK, H , I, J,... → B cascade bands in the middle ultraviolet 200-500 nm. At 19 eV the total of emission cross sections for these band systems observed by James et al. was about 1.3×10^{-18} cm^2. The latter study represents a lower limit, since another 10-20% of the band systems emissions lie longward of 500 nm. Therefore, we estimate from this study that the EF state must produce about 80-90% of the intensity of the cascading band systems.

One further step in the study of the EF cross sections was accomplished at 100 eV. The regression analysis showed that the cascade cross section at 100 eV was 5.0×10^{-18} cm^2. The 100 eV cross section for the B-X cascade is 70 % larger than the previous value of 2.9×10^{-18} cm^2 recommended by Ajello et al. (1988). This value can be compared to 2.6×10^{-17} cm^2 for the B-X direct excitation cross section (Liu et al., 1998). The cascade cross section falls by a factor of 3.4 from 20 to 100 eV. The fall-off in cross section from 20 to 100 eV is matched by our earlier estimates (Ajello et al.,1984; Shemansky et al., 1985).

In conclusion, we showed that a pulsed gun technique can operate in 3 modes in the time domain to directly measure: 1) cascade spectra, 2) energy dependence of cascade cross sections (not shown here) or 3) effective cascade lifetimes for resonance transitions in the UV. Comparing the cascade and directly excited spectra to the DC spectrum, the cascade cross section can be determined.

The research described in this paper was carried out at the Jet Propulsion Laboratory, California Institute of Technology, and was sponsored by the U.S. Air Force Office of Scientific Research (AFOSR), the Aeronomy Program of the National Science

foundation (ATM-9320589) and NASA Planetary Atmospheres and UV, Visible and Gravitational Astrophysics. D.D. is supported by the National Research Council.

REFERENCES

H. Abgrall and E. Roueff, Astron. Astrophys., **79**, 313 (1989).

H. Abgrall, et al., Can. J. Phys., **72**, 856 (1994).

J. M. Ajello et al., J. Geophys. Res., **103**, 20125 (1998).

J. M. Ajello, et al., Appl. Opt., **27**, 890 (1988).

J. M. Ajello, et al., Phys. Rev. A., **29**, 636 (1984).

A. L. Broadfoot et al., J. Geophys. Res. **86**, 8259 (1981).

A. L. Broadfoot et al., Science **246**, 1459 (1989).

D. W. Chandler and L. Thorne, J. Chem. Phys. **85**, 1733 (1986).

M. Glass-Maujean et al., Phys. Rev. A, **28**, 2868 (1983).

M. Glass-Maujean et al., J. Chem. Phys. **80**, 4355(1984).

K. P. Huber and G. Herzberg, Molecular Spectra and Molecular Structure: IV, Constants of Diatomic Molecule (Van Nostrand, New York, 1979) p 250.

G. K. James, J. M. Ajello, J and W. Pryor, J. Geophys. Res. **103**, 20113 (1998).

C. Jonin et al., Ap. J. Supp. (In Press, 1999).

M. Khakoo, D. Roundy, and F. Rugamas, Phys. Rev. A **54**, 4004 (1996).

X. Liu, et al., Ap. J., **101**, 375 (1995).

X. Liu, et al., J. Geophys. Res. **103**, 26739 (1998).

R. Meier, Space. Sci. Rev., **85**, 18960 (1991).

E. W. McDaniel, Atomic Collisions (Wiley Interscience Publications, 1989) p.330.

J. C. Raymond, W. P.Blair, and K. S.Long, , Ap. J., **489**, 314 (1997).

J.-Y. Roncin and F. Launay, Atlas of the Vacuum Ultraviolet Emission Spectrum of Molecular Hydrogen (J. Phys. Chem. Ref. Data Monogr. **4**, Woodbury, NY, 1994).

D. E., Shemansky, J. M. Ajello and D. T. Hall, Ap. J. **296**, 765 (1985).

R. J. Spindler, J. Quant. Spectrosc. Radiat. Transfer, **9**, 1041 (1969).

K. Tsukiyama, J. Ishii, J. and T. Kasuya, J. Chem. Phys., **97**, 875 (1992).

J. Watson, J. and R. J. Anderson, J. Chem. Phys. **66**, 4025 (1977).

L. Wolniewicz and K. J. Dressler, J. Chem. Phys. **100**, 444 (1994).

TABLE OF FIGURES

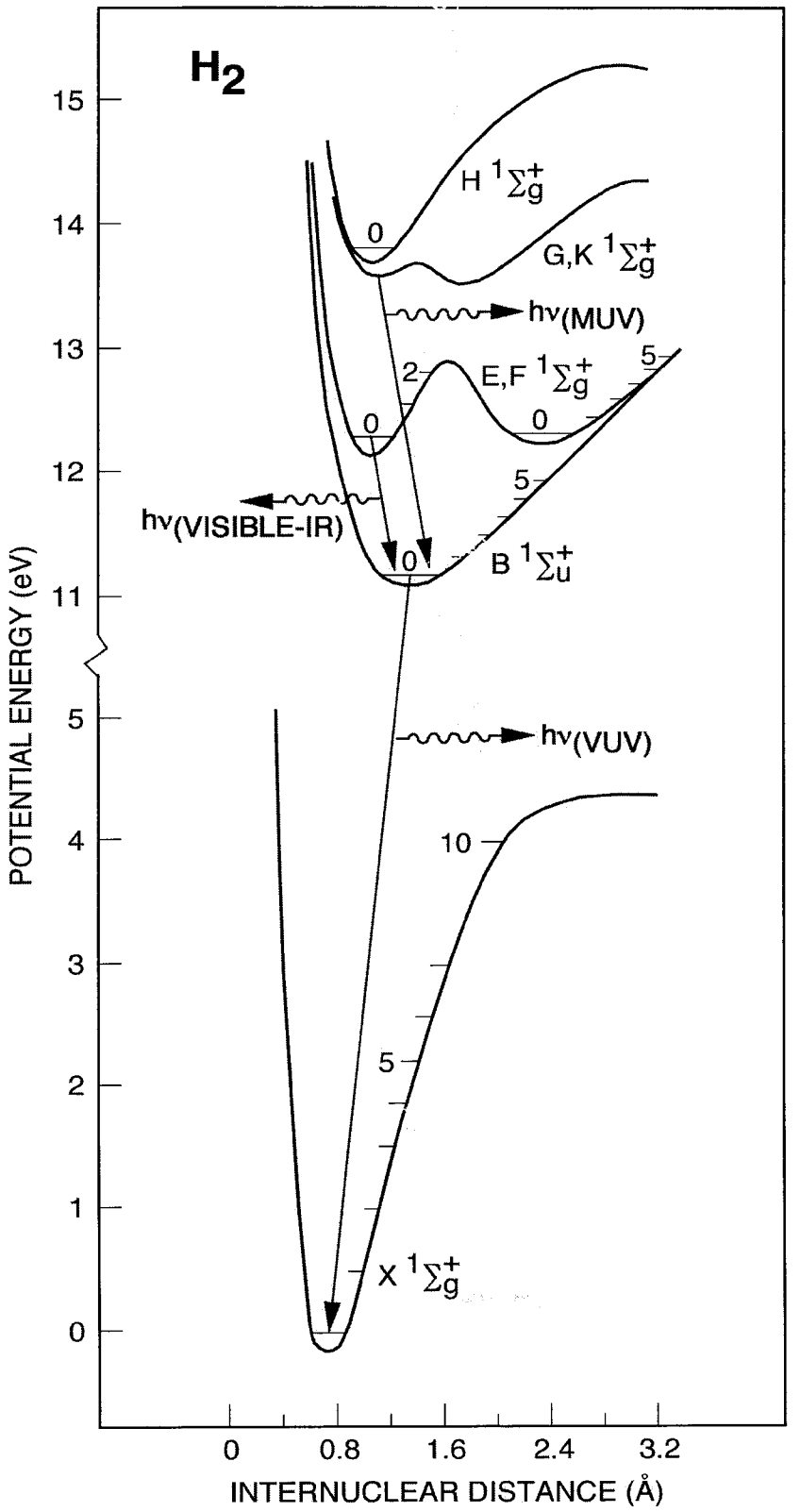
H2
H 1Σg+
G,K 1Σg+
hν(MUV)
E,F 1Σg+
hν(VISIBLE-IR)
B 1Σu+
hν(VUV)
X 1Σg+
POTENTIAL ENERGY (eV)
INTERNUCLEAR DISTANCE (Å)
0
0.8
1.6
2.4
3.2
15
14
13
12
11
5
4
3
2
1
0

FIG. 1

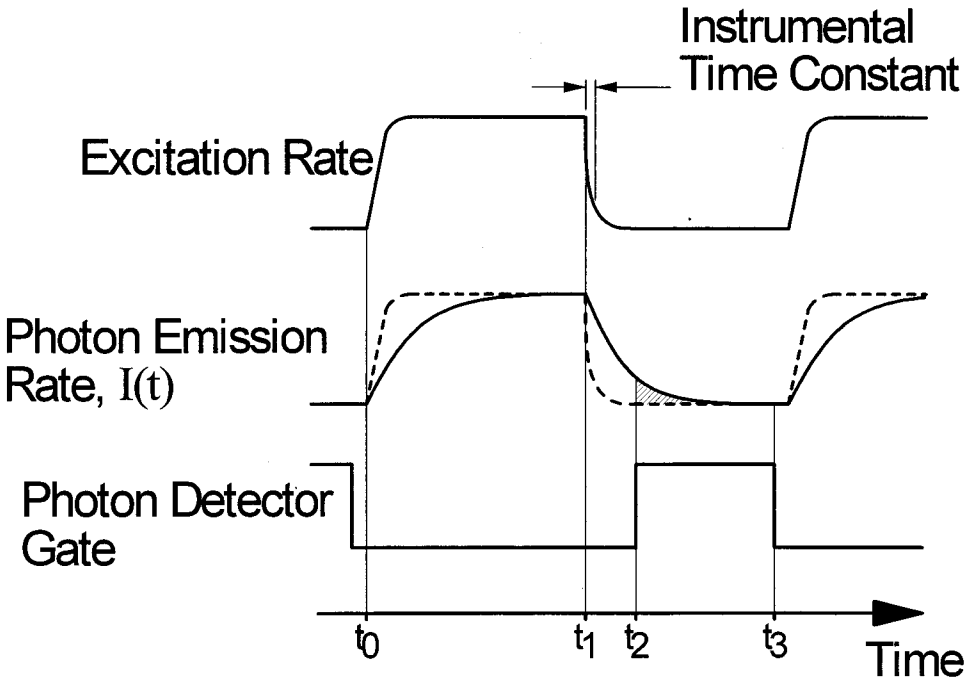
Instrumental
Time Constant
Excitation Rate
Photon Emission
Rate, I(t)
Photon Detector
Gate
t0
t1
t2
t3
Time

FIG. 2

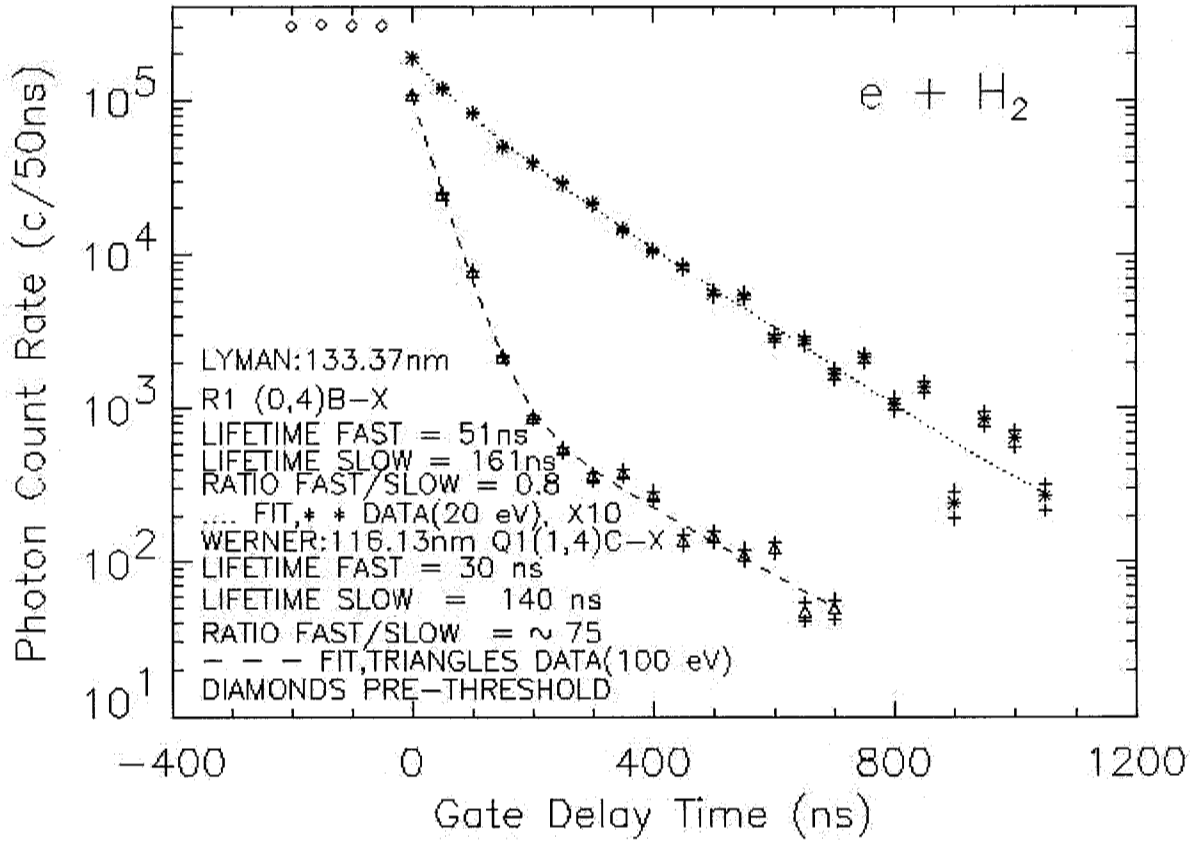
e + H_2
LYMAN:133.37nm
R1 (0,4)B−X
LIFETIME FAST = 51ns
LIFETIME SLOW = 161ns
RATIO FAST/SLOW = 0.8
.... FIT,* * DATA(20 eV), X10
WERNER:116.13nm Q1(1,4)C−X
LIFETIME FAST = 30 ns
LIFETIME SLOW = 140 ns
RATIO FAST/SLOW = ~ 75
− − − FIT,TRIANGLES DATA(100 eV)
DIAMONDS PRE−THRESHOLD
Photon Count Rate (c/50ns)
10^5
10^4
10^3
10^2
10^1
−400
0
400
800
1200
Gate Delay Time (ns)

FIG. 3

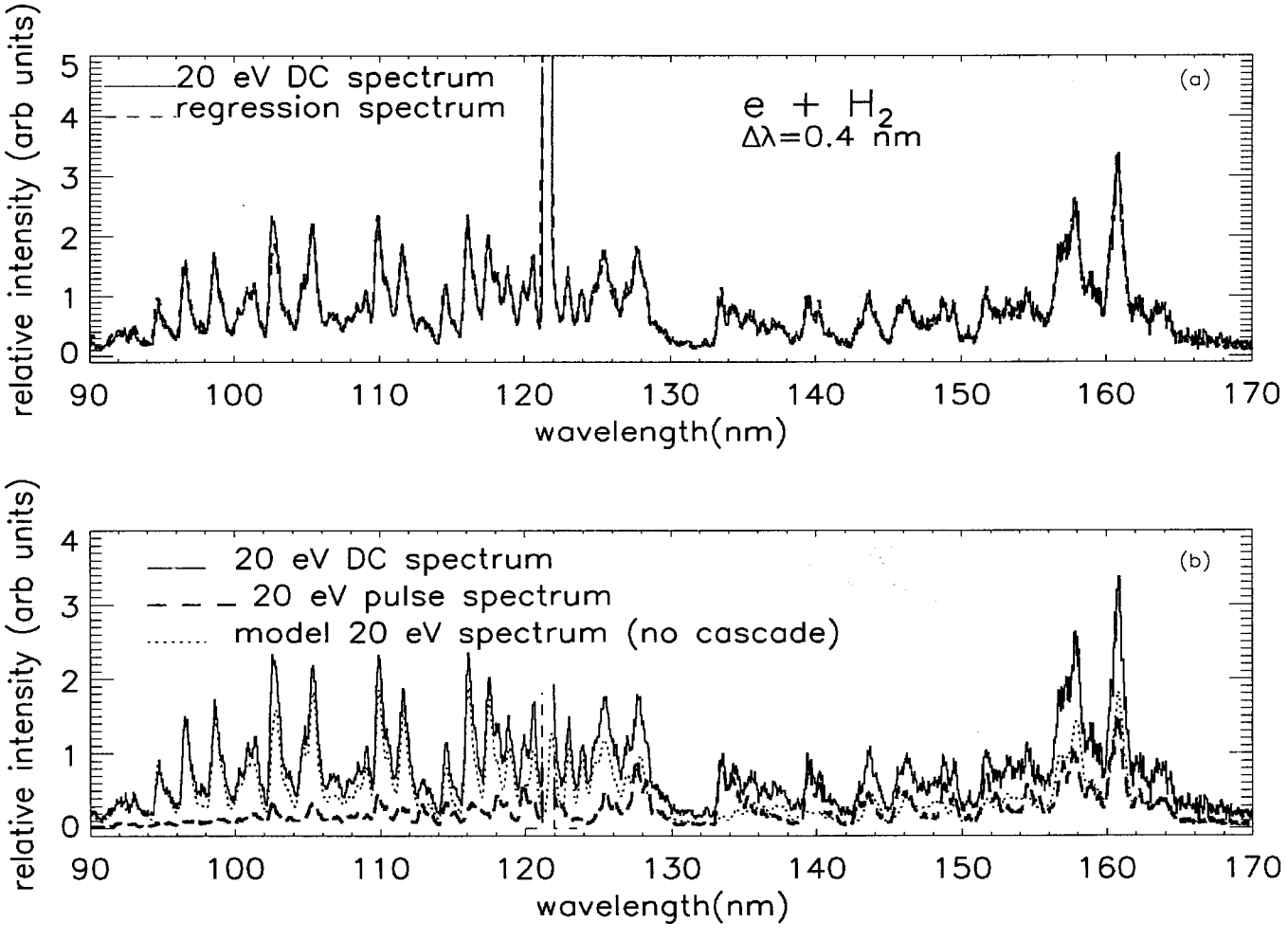
relative intensity (arb units)
20 eV DC spectrum
regression spectrum
e + H2
Δλ=0.4 nm
(a)
wavelength(nm)
relative intensity (arb units)
20 eV DC spectrum
20 eV pulse spectrum
model 20 eV spectrum (no cascade)
(b)
wavelength(nm)

FIG. 4